



PCCP

Impact of iodine loading and substitution position on intersystem crossing efficiency in a series of ten methylated-mesophenyl-BODIPY dyes

Journal:	<i>Physical Chemistry Chemical Physics</i>
Manuscript ID	CP-ART-11-2020-005904.R1
Article Type:	Paper
Date Submitted by the Author:	16-Apr-2021
Complete List of Authors:	Ly, Jack; Air Force Research Laboratory Materials and Manufacturing Directorate; UES Inc Presley, Kayla; Air Force Research Laboratory Materials and Manufacturing Directorate, RXAP Cooper, Thomas; Air Force Research Laboratory Materials and Manufacturing Directorate, Baldwin, Luke; Air Force Research Laboratory Materials and Manufacturing Directorate Dalton, Matthew; Air Force Research Laboratory Materials and Manufacturing Directorate Grusenmeyer, Tod; Air Force Research Laboratory Materials and Manufacturing Directorate

SCHOLARONE™
Manuscripts

Impact of iodine loading and substitution position on intersystem crossing efficiency in a series of ten methylated-*meso*-phenyl-BODIPY dyes

Jack T. Ly^{a,b}, Kayla F. Presley^a, Thomas M. Cooper^a, Luke A. Baldwin^a, Matthew J. Dalton^a, and Tod A. Grusenmeyer^a

^a*Air Force Research Laboratory, Materials and Manufacturing Directorate, Wright-Patterson Air Force Base, Dayton, Ohio 45433, United States*

^b*UES, Inc., Dayton, Ohio 45432, United States*

Four core and six distyryl-extended methylated-*meso*-phenyl-BODIPY dyes with varying iodine content were synthesized. The influence of iodine loading and substitution position on the photophysical properties of these chromophores was evaluated. Selective iodine insertion at the 2- and 6- positions of the methylated-*meso*-phenyl-BODIPY core, rather than maximum iodine content, resulted in the highest intersystem crossing efficiency. Iodination of the distyryl-extended BODIPY core afforded intersystem crossing quantum yields comparable to 2,6-diiodo-BODIPY. Inclusion of an iodine at the *para-meso*-phenyl position generally enhanced non-radiative decay in the BODIPY excited-state, leading to lower fluorescence and intersystem crossing quantum yield values. Iodine substitution at the styryl-positions resulted in negligible changes to the excited-state dynamics. This study highlights: (1) the rate of radiative decay is similar in all ten derivatives (on the order of $1 \times 10^8 \text{ s}^{-1}$), (2) iodination of the 2,6-positions results in the greatest enhancement of intersystem crossing efficiency, (3) care must be taken when modifying the *para-meso*-phenyl position as it could have detrimental effects on the excited-state dynamics, (4) the excited-state is negligibly affected by iodination of the styryl groups, potentially enabling orthogonal functionalization without modifying the molecular photophysics, (5) distyryl extension of the chromophore core diminishes rates of non-radiative decay and intersystem crossing, resulting in higher fluorescence quantum yields and lower intersystem crossing yields in the π -extended derivatives compared to the core BDP derivatives, and (6) DFT calculations provide insight into the electronic and structural factors regulating intersystem crossing and vibrational relaxation in these molecules.

Boron-dipyrromethane (BODIPY or BDP) chromophores are extremely popular due to their photostability, high molar absorptivity, exemplary luminescence quantum yields, and excellent absorption and emission tunability in the visible and near-infrared (NIR) regimes.¹⁻³ Increased interest in developing BODIPY-based photosensitizer and fluorescent probes has garnered multiple synthetic and application review articles in recent years.^{2,4-17} Much attention has been directed toward the synthesis of BODIPY chromophores with high intersystem crossing efficiencies for use in a variety of applications, such as triplet-triplet annihilation up-conversion (TTA-UC)^{12,18-23}, singlet oxygen formation for photodynamic therapy (PDT),^{4-6,10,11,15-17} and photocatalysts for H₂ production and organic photoredox reactions.^{12,24-26} Modulation of the intersystem crossing efficiency has been demonstrated using a variety of synthetic strategies,

including the installation of heavy-atoms,^{10,27–29} the use of orthogonally oriented bisBODIPYs^{13,18,30–32} or fullerene conjugates,^{7,33–37} and the utilization of intramolecular photoinduced electron transfer inducing motifs.^{8,9,12} These synthetic approaches result in intersystem crossing efficiencies that are highly variable and depend on the location and chemical nature of the substituents.

Two strategies are generally employed when constructing heavy-atom containing BODIPY chromophores for triplet-state sensitization: (1) incorporation of a transition metal complex in the *para-meso*-phenyl or 2,6- positions of the BODIPY core or (2) direct substitution of halides onto the BODIPY core. Bipyridines conjugated via an acetylene bridge at both the 2,6- and *para-meso*-phenyl positions have been reported for triplet sensitization in cyclometalated Ru(II), Ir(II), and Re(I) adducts.^{14,20,38–42} Other chelating moieties to cyclometalated Ir(II) adducts, such as cyanamide and acetylacetonate, have shown appreciably high triplet yields.^{43,44} More recently, Choung *et al.* reported a BODIPY chromophore with dual luminescence through modulation of an iridium ancillary ligand directly chelated to the pyridyl-substituent at the *meso*-position.⁴⁵ Reports of direct attachment of transition metals to the BODIPY core is mostly limited to Pt(II) analogues directly coupled at the *meso*-core or covalently bound to the 2,6-positions via acetylene bridges.^{19,21,22,25,46–48} Similar direct conjugation of Au(I) and Au(III) adducts has been reported with limited description of their intersystem crossing efficiencies.^{23,49,50}

Compared to metal containing derivatives, incorporation of iodine or bromine in BODIPY dyes provides an easily accessible, effective approach to achieve intersystem crossing efficiencies comparable to metalated dyes through the heavy-atom effect. Halogenated BODIPYs require a one-step reaction from commercially available starting materials, whereas metalated dyes commonly require multi-step syntheses. Iodines are commonly chosen as the iodo-adducts consistently outperform brominated BODIPYs for ¹O₂ sensitization, because ISC/triplet formation is more efficient with the heavier halide.^{10,27} Furthermore, Ortiz *et al.* demonstrated that increasing iodine content from 2,6-diiodo- to 2,3,5,6-tetraiodo- *meso*-phenyl-BODIPY modestly enhanced ¹O₂ quantum yield from 83% to 87%.²⁸ Iodination beyond the dipyrroin core at the periphery aryls in aza-BODIPY has also been shown to produce higher triplet yields (86%) compared to iodination at the core 2,6-positions alone (68%).²⁹ Although these previous reports on transition metal and halide substituted BODIPYs describe the presence of triplet excited-states, complete excited-state characterization enabling a comparison of molecular structure with the radiative, non-radiative, and intersystem crossing rate constants is generally underreported.

There has yet to be a definitive investigation on the impact of iodine loading and substitution position on the photophysical properties of the popular methylated, *meso*-phenyl substituted BODIPY subclass. These BODIPY derivatives possess relatively long fluorescence lifetimes (≥ 1 ns) and relatively high fluorescence quantum yields (≥ 0.40) due to steric hindrance at the *meso*-position.⁵¹ Additionally, the resultant rate of radiative decay, which is on the order of 10^8 s⁻¹, is slow enough for heavy-atom-induced intersystem crossing to influence the excited-state

dynamics. With this in mind, we investigated the impact of iodine loading and substitution position on the intersystem crossing efficiency in a library of four core and six distyryl-extended methylated-*meso*-phenyl-BODIPYs,^{24,34,52–55} including two previously unreported BODIPYs. Iodine loading and location were varied among the *para-meso*-phenyl position, the 2,6-positions, and the *para*-styryl-positions with the latter only being applicable to the distyryl-extended BODIPYs. All ten derivatives were characterized using a combination of steady-state and time-resolved spectroscopy. The fluorescence lifetime, fluorescence quantum yield, and intersystem crossing quantum yield for each molecule was determined, enabling the calculation of the radiative, non-radiative, and intersystem crossing rate constants. DFT calculations were performed in order to provide insight into the electronic and structural factors governing the excited-state dynamics in these chromophores. This detailed study evaluating rate constants as a function of structural modification offers valuable information for the rational design of functional BODIPYs.

Results and Discussion

The molecular structures of the four core and six distyryl-extended methylated, *meso*-phenyl-BODIPYs are presented in **Figure 1**. Molecular structure labeling follows an I_n -BDP- m nomenclature convention where the “ n ” subscript indicates the number of iodine atoms positioned on the methylated-*meso*-phenyl-BODIPY portion of the molecule, and the “ m ” numeral refers to the number of iodine atoms present on the styryl extensions. Detailed synthetic procedures, as well as the methodology used in the collection and calculation of all of the photophysical data, are outlined in the supporting information. Briefly, iodination of the core **BDP** and **I-BDP** parent dyes was afforded via stirring with N-iodosuccinimide in methylene chloride at ambient temperature for **BDP** and iodic acid/ I_2 in ethanol at 70 °C for **I-BDP** (see SI). Distyryl-BDPs were synthesized through Knoevenagel condensation with the appropriate aryl aldehydes in DMF/THF solvent. Knoevenagel distyryl-products from **I₃-BDP** were attempted, but due to solubility issues, confirmation of structure and purity of target molecules **I₃-BDP-0** and **I₃-BDP-2** (see SI) was not possible, and thus, those derivatives were not included in this study. All other BDP dyes were confirmed via ¹H NMR and high resolution LDI-MS. For ease of discussion, the chromophores have been organized into three groups: the core BDPs, the non-triplet yielding distyryl-BDPs, and triplet yielding distyryl-BDPs. Within these groups, the photophysical properties of the molecules are discussed in terms of increasing iodine content. Shifts in the ground-state absorption and steady-state luminescence spectra of the molecules are compared in units of eV to aid in the comparison of energy shifts across a broad wavelength range.

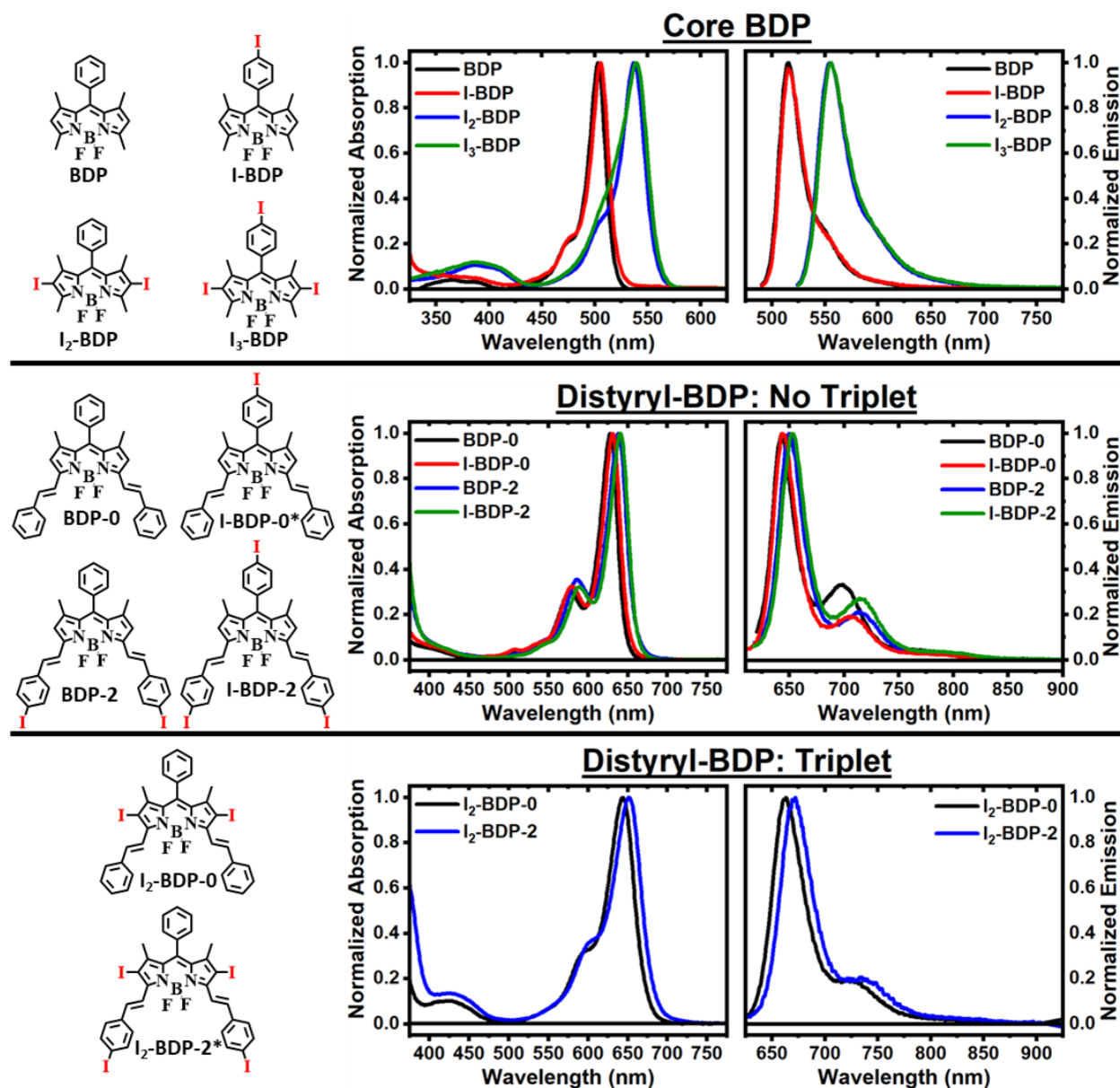


Figure 1. Molecular structures, along with normalized absorption and emission spectra in toluene at room temperature, of (top) core BDPs, (middle) non-triplet forming distyryl-BDPs, and (bottom) triplet forming distyryl-BDPs. Molecules are ordered within their respective group by increasing iodine content. *Denotes previously unreported derivative.

Ground-State Absorption and Steady-State Fluorescence and Phosphorescence Spectra

The normalized ground-state absorption and steady-state fluorescence spectra of all ten BDPs collected in toluene are shown in **Figure 1**, and 77 K phosphorescence spectra of the core BDP derivatives in 2:2:1:1 (v:v) ethyl iodide, diethyl ether, ethanol, toluene (EEET) glass are shown in **Figure 2**. Relevant ground-state absorbance and steady-state emission properties are listed in **Table 1**. Overlays of the excitation spectrum collected at the low energy shoulder or maximum

of the 0-1 transition in the fluorescence spectrum with the normalized ground-state absorption spectrum of each complex are provided in **Figures S23-25**. Superposition of the excitation spectra with the ground-state absorption spectra provides confidence that the observed luminescence results from the designated BODIPY derivative and not an impurity. The ground-state absorption spectra for all the compounds are highly structured, indicating π - π^* character.⁵⁶ The lowest energy ground-state absorption maximum for the parent core BODIPY (**BDP**) is observed at 2.47 eV (503 nm). A single iodine atom in the *para*-position of the *meso*-phenyl group (**I-BDP**) induces a subtle bathochromic shift in the lowest energy ground-state absorption maximum to 2.46 eV (505 nm). Upon iodination at the 2,6-positions, the lowest energy ground-state absorption maximum of **I₂-BDP** (2.31 eV, 537 nm) is red-shifted relative to **BDP** (2.47 eV, 503 nm) by 0.16 eV. A similar 0.16 eV shift is also observed when comparing the lowest energy ground-state absorption maximum of **I₃-BDP** (2.30 eV, 539 nm) to **I-BDP** (2.46 eV, 505 nm). Again, a minimal 0.01 eV bathochromic shift is observed in the lowest energy ground-state absorption maximum of **I₃-BDP** (2.30 eV, 539 nm) when compared with **I₂-BDP** (2.31 eV, 537 nm). The ground-state molar absorptivity values ($\epsilon_{\lambda_{\max}}$) obtained for the core BDP derivatives are similar and range from 76,000-82,000 M⁻¹ cm⁻¹. These values are in agreement with previous literature reports.^{7,17,26,53,57,58}

Table 1. Ground-state absorbance and steady-state emission properties of BDP dyes studied.

		$\epsilon_{\lambda_{\max}}$ (M cm) ⁻¹	λ_{Abs} , nm (eV)	λ_{FL} , nm (eV)	λ_{PHOS} , nm (eV)	ΔE_{ST} (eV)
Core BDP	BDP	76 x 10 ³	503 (2.47)	515 (2.41)	755 (1.64) ^A	0.77
	I-BDP	82 x 10 ³	505 (2.46)	519 (2.39)	761 (1.63) ^A	0.76
	I₂-BDP	82 x 10 ³	537 (2.31)	555 (2.23)	756 (1.64) ^A	0.59
	I₃-BDP	80 x 10 ³	539 (2.30)	562 (2.21)	761 (1.63) ^A	0.58
Distyryl-BDP No Triplet	BDP-0	115 x 10 ³	628 (1.97)	643 (1.93)	NA ^B	NA ^B
	I-BDP-0	93 x 10 ³	631 (1.97)	644 (1.93)	NA ^B	NA ^B
	BDP-2	122 x 10 ³	639 (1.94)	650 (1.91)	NA ^B	NA ^B
	I-BDP-2	101 x 10 ³	641 (1.93)	652 (1.90)	NA ^B	NA ^B
Distyryl-BDP Triplet	I₂-BDP-0	92 x 10 ³	644 (1.93)	663 (1.87)	NA ^B	NA ^B
	I₂-BDP-2	113 x 10 ³	652 (1.90)	672 (1.85)	NA ^B	NA ^B

All data collected in room temperature toluene unless otherwise noted. Legend: $\epsilon_{\lambda_{\max}}$ = molar absorptivity at maximum absorption; λ_{Abs} = peak absorption wavelength; λ_{FL} = peak fluorescence wavelength and energy; λ_{PHOS} = peak phosphorescence wavelength and energy; ΔE_{ST} = singlet-triplet energy gap; NA = unable to acquire specified

data. ^AData collected in 2:2:1:1 (v:v) ethyl iodide, diethyl ether, ethanol, toluene (EEET) glass at 77 K. ^BUnable to observe phosphorescence from any distyryl-extended derivative in EEET glass at 77 K. We attempted to locate signal on both Vis and NIR PMTs using steady-state and gated acquisition modes.

Expansion of the dipyrin core with styryl moieties at the 3- and 5- methylene positions results in a bathochromic shift of the lowest energy ground-state absorption maxima into the 1.97-1.89 eV (mid-600 nm) range. For the π -extended distyryl-BDP series, bathochromic shifts induced by iodine substitution are modest when compared with the non-extended, core BDP chromophores. The lowest energy ground-state absorption maximum for the parent π -extended distyryl-BDP (**BDP-0**) occurs at 1.97 eV (628 nm). Installation of an iodine atom in the *para*-position of the *meso*-phenyl group has a minimal impact on the lowest energy ground-state absorption maximum of **I-BDP-0** (1.97 eV, 631 nm). Distyryl-BDPs with iodination at the *para*-styryl periphery versus those without (**BDP-2** versus **BDP-0** and **I-BDP-2** versus **I-BDP-0**) exhibit an approximately 0.04 eV (~ 10 nm) bathochromic shift in their lowest energy ground-state absorption maxima. The inclusion of an iodine atom in the *para*-position of the *meso*-phenyl group once again results in a slight bathochromic shift in the longest wavelength ground-state absorption maximum of **I-BDP-2** (1.93 eV, 641 nm) relative to **BDP-2** (1.94 eV, 639 nm). The observed shifts in longest wavelength ground-state absorption maxima of the π -extended distyryl-BDP derivatives are also less dramatic than the core BDP derivatives upon incorporation of iodine atoms in the 2,6-positions. A minimal 0.04 eV bathochromic shift is observed upon iodination at the 2,6-positions of the π -extended distyryl-BDP derivatives (**I₂-BDP-0** versus **BDP-0** and **I₂-BDP-2** versus **BDP-2**). Compared to the core BDPs, a notable increase in $\epsilon_{\lambda_{\max}}$ is observed upon π -extension in all derivatives. Additionally, there is some variability in the calculated molar absorptivity values of the iodine containing π -extended distyryl-BDP derivatives. For example, **BDP-0** and **I₂-BDP-0** exhibit $\epsilon_{\lambda_{\max}}$ values of 115,000 and 92,000 M⁻¹ cm⁻¹, while the molar absorptivities of **BDP-2** and **I₂-BDP-2** are 122,000 and 113,000 M⁻¹ cm⁻¹, respectively. The enhancement in the molar absorptivity values upon π -extension of the BDP core has been broadly observed in the literature.^{24,34,52-55} A roughly 20% variability in the molar absorptivity values of the iodine substituted derivatives is also in agreement with previous literature reports.^{10,27-29,51} The observed trends in the lowest energy ground-state absorption maximum and molar absorptivity values are also supported by singlet-state energies and oscillator strength values obtained from DFT calculations (**Table S11**).

The fluorescence spectra of all ten molecules possess vibronic structure in room temperature toluene solution. This structure is subtle in the core BDP derivatives, appearing as a shoulder on the red edge of the 0-0 transition. The vibronic structure is more pronounced in the fluorescence spectra of the distyryl-extended BODIPYs; the 0-1 transition is resolved in all of the π -extended derivatives. Small Stokes shifts are also observed in all ten derivatives. This combination of structured fluorescence spectra and small Stokes shifts is reflective of the π - π^* nature of the fluorescence. The observed trends in the fluorescence maxima are similar to those observed for the ground-state absorption maxima. Inclusion of an iodine atom in the *para*-position of the *meso*-phenyl group results in minimal bathochromic shifts in the fluorescence maxima of **I-BDP**

(2.39 eV, 519 nm) when compared to the unsubstituted **BDP** (2.41 eV, 515 nm) and in **I₃-BDP** (2.21 eV, 562 nm) when compared to **I₂-BDP** (2.23 eV, 555 nm). Iodination of the BDP core results in a larger 0.18 eV bathochromic shift in the fluorescence maxima of **I₃-BDP** (2.21 eV, 562 nm) and **I₂-BDP** (2.23 eV, 555 nm). The addition of the distyryl moieties shifts the fluorescence maxima into the 1.93-1.84 eV (640-675 nm) range. Inclusion of an iodine at the *para-meso*-phenyl position has minimal effects on the fluorescence maxima with **I-BDP-0** and **I-BDP-2** both experiencing a ≤ 0.01 eV (≤ 2 nm) difference in their fluorescence maxima relative to **BDP-0** and **BDP-2**, respectively. Iodination at the 2,6- and *para*-styryl positions in the π -extended distyryl-BDP derivatives resulted in modest bathochromic shifts (0.02-0.06 eV) in the fluorescence maxima compared to 2,6-iodination of the core BDPs (0.18 eV). 2,6-iodination of the π -extended distyryl-BDP derivatives leads to greater bathochromic shifts in fluorescence maxima compared to *para*-styryl iodination. Correspondingly, the lowest energy fluorescence maximum is observed for **I₂-BDP-2** with 2,6- and *para*-styryl substitution (1.85 eV, 672 nm).

Steady-state phosphorescence spectra of the four core BDP derivatives, **BDP**, **I-BDP**, **I₂-BDP**, and **I₃-BDP**, were collected in 2:2:1:1 (v:v) ethyl iodide, diethyl ether, ethanol, toluene (EEET) glass at 77 K. The use of iodine containing solvents in low temperature glasses is known to facilitate phosphorescence via an external heavy atom effect.^{59,60} All four low temperature phosphorescence spectra possess vibronic structure, leading to the conclusion that the phosphorescence is also π - π^* in nature in the core BDP derivatives. The phosphorescence maxima of the core BDP derivatives fall between 755 nm and 761 nm. This represents a < 0.01 eV energy difference in the triplet excited-state energies of these chromophores. This similarity in triplet excited-state energies amongst the core BDP derivatives leads to an interesting trend in the singlet-triplet energy gaps (ΔE_{ST}) of **BDP**, **I-BDP**, **I₂-BDP**, and **I₃-BDP**; the non-2,6-diiodo substituted derivatives, **BDP** and **I-BDP**, possess significantly larger singlet-triplet energy gaps than the 2,6-diiodo substituted derivatives, **I₂-BDP** and **I₃-BDP**. We also attempted to collect the 77 K phosphorescence spectra of the distyryl-extended derivatives. Unfortunately, no discernable phosphorescence was detected for any of these derivatives despite attempts to locate signal on both our VIS and NIR PMTs while using steady-state and time-gated acquisition modes.

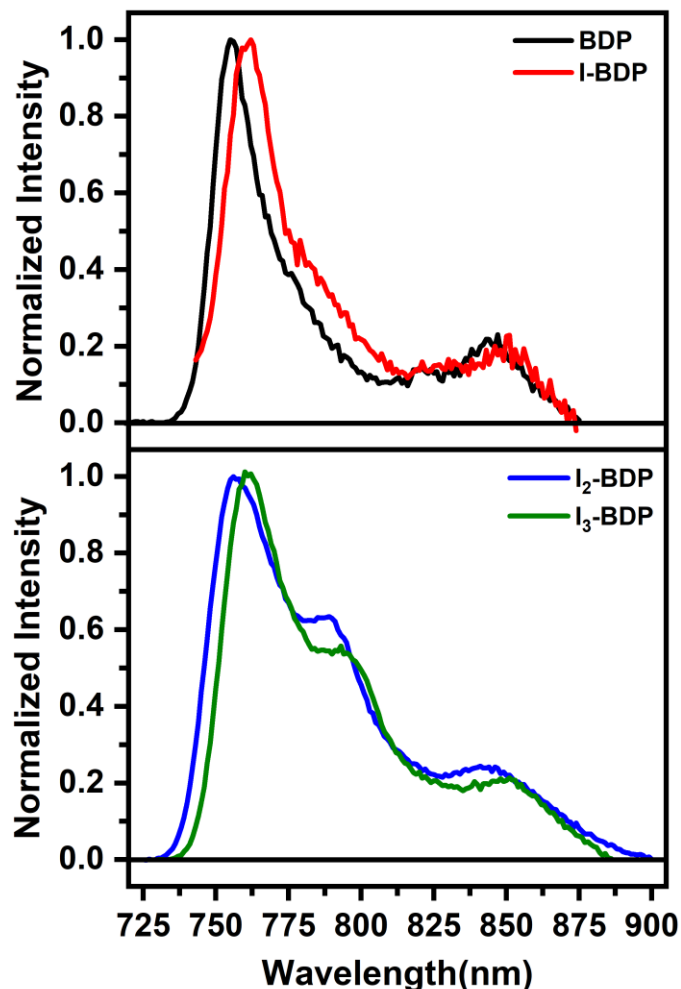


Figure 2. Phosphorescence spectra of (top) non-2,6-iodinated chromophores, **BDP** and **I-BDP**, and (bottom) 2,6-iodinated chromophores, **I₂-BDP** and **I₃-BDP**. The data was collected in 2:2:1:1 (v:v) ethyl iodide, diethyl ether, ethanol, toluene (EEET) glass at 77 K.

Excited-State Dynamics

To investigate the impact of iodo-position and loading upon the excited-state dynamics, fluorescence lifetime (τ_s), fluorescence quantum yield (ϕ_F), and intersystem crossing quantum yield (ϕ_T) experiments were conducted on all 10 compounds in toluene solution. Representative fluorescence lifetime decays for **BDP** and **I₂-BDP** as well as photosensitized singlet oxygen phosphorescence spectra from absorbance matched samples of **I₂-BDP**, **I₃-BDP**, **I₂-BDP-0**, and **I₂-BDP-2** are shown in **Figure 3**. Relevant fluorescence lifetime decay curves (**Figures S26-S28**), fluorescence quantum yield spectra (**Figures S29-S31**), and singlet oxygen phosphorescence quantum yield spectra (**Figures S32-S34**) are provided in the supporting information. The collection of this data allowed for the determination of the radiative decay rate constant (k_r), the non-radiative decay rate constant (k_{nr}), and the intersystem crossing rate constant (k_{ISC}). Results

of these experiments and the calculated rate constants are summarized in **Table 2**. The system of equations used to determine these rate constants are shown in Equations S2-S4.

Table 2. Summary of BDP photophysical properties in this study.

		τ_s (ns)	ϕ_F	ϕ_T	k_r (s ⁻¹)	k_{nr} (s ⁻¹)	k_{isc} (s ⁻¹)
Core BDP	BDP	3.80 ± 0.20	0.45 ± 0.02	- ^a	1.2E+08	1.5E+08	- ^a
	I-BDP	3.20 ± 0.10	0.44 ± 0.03	- ^a	1.4E+08	1.8E+08	- ^a
	I₂-BDP	0.24 ± 0.05	0.03 ± 0.01	0.84 ± 0.04	1.3E+08	5.4E+08	3.5E+09
	I₃-BDP	0.21 ± 0.03	0.03 ± 0.01	0.81 ± 0.07	1.4E+08	7.6E+08	3.9E+09
Distyryl-BDP No Triplet	BDP-0	5.80 ± 0.80	0.84 ± 0.05	- ^a	1.4E+08	2.8E+07	- ^a
	I-BDP-0	5.80 ± 1.30	0.71 ± 0.08	- ^a	1.2E+08	5.0E+07	- ^a
	BDP-2	5.50 ± 1.30	0.81 ± 0.01	- ^a	1.5E+08	3.5E+07	- ^a
	I-BDP-2	5.60 ± 1.40	0.73 ± 0.06	- ^a	1.3E+08	4.8E+07	- ^a
Distyryl-BDP Triplet	I₂-BDP-0	1.70 ± 0.10	0.23 ± 0.01	0.76 ± 0.04	1.3E+08	5.9E+06	4.5E+08
	I₂-BDP-2	1.70 ± 0.10	0.22 ± 0.01	0.78 ± 0.03	1.3E+08	- ^b	4.6E+08

All data collected in room temperature toluene. Legend: τ_s = fluorescence lifetime measured from time-correlated single-photon counting; ϕ_F = fluorescence quantum yield; ϕ_T = intersystem crossing quantum yield; k_r = radiative decay rate constant; k_{nr} = non-radiative decay rate constant; k_{isc} = intersystem crossing rate constant. ^aNot able to be measured/calculated. ^bNot able to be calculated because $\phi_F + \phi_T = 1$. Molecules are ordered within respective groups by increasing iodine content.

The excited-state dynamics of the core BODIPY dyes are greatly influenced by the number and position of the iodine substituents. **BDP** and **I-BDP** have nearly identical fluorescence quantum yields (0.44 and 0.45, respectively) and do not appear to form triplet excited-states upon excitation). The fluorescence lifetime of **I-BDP** (3.20 ns) is quantitatively shorter than **BDP** (3.80 ns). Iodination at the *para-meso*-phenyl position of **I-BDP** resulted in a roughly 20% percent increase in the both the radiative and non-radiative decay rate constants relative to **BDP**. Installation of iodine atoms in the 2- and 6- positions dramatically affects the excited-state dynamics of the core BDPs. The fluorescence quantum yields of the 2,6-substituted derivatives, **I₃-BDP** (0.03) and **I₂-BDP** (0.03), are more than an order of magnitude lower than those of the non-2,6-substituted derivatives, **I-BDP** (0.45) and **BDP** (0.44). The fluorescence lifetime values collected for **I₃-BDP** (0.21 ns) and **I₂-BDP** (0.24 ns) are also an order of magnitude shorter than those observed for **I-BDP** (3.20 ns) and **BDP** (3.80 ns). Significant photosensitized singlet oxygen phosphorescence is observed in solutions of **I₃-BDP** and **I₂-BDP**, yielding intersystem crossing quantum yield values of 0.81 and 0.84, respectively. Inclusion of iodine atoms at the 2- and 6- positions greatly enhances the rate of intersystem crossing; in fact, this happens to such an extent

that intersystem crossing becomes the dominant kinetic pathway with k_{ISC} ($\sim 4 \times 10^9 \text{ s}^{-1}$) being almost an order of magnitude larger than both k_r ($\sim 1 \times 10^8 \text{ s}^{-1}$) and k_{nr} ($\sim 5 \times 10^8 \text{ s}^{-1}$). Iodination at the *para-meso*-phenyl position again appears to enhance non-radiative decay from the singlet excited-state as k_{nr} of **I₃-BDP** ($7.6 \times 10^8 \text{ s}^{-1}$) is appreciably higher than **I₂-BDP** ($5.4 \times 10^8 \text{ s}^{-1}$). The additional *para-meso*-phenyl iodine beyond the 2,6-positions does not enhance the rate of intersystem crossing. This effect is likely due to a near perpendicular orientation of the *meso*-phenyl substituent to the dipyrin core fixed between the spatially adjacent 1,7-methylenes as shown in previously reported crystal structures.^{47,61} This orthogonal orientation of the *meso*-phenyl substituent prohibits iodine from accessing the π orbitals of the BDP core, preventing an enhancement in the rate of intersystem crossing, while enabling and enhancing non-radiative modes of decay from the excited-state as evidenced by increased k_{nr} . Furthermore, this orientation helps to rationalize the negligible effect of the *para-meso*-phenyl iodine on the ground-state absorption and fluorescence maxima of these molecules.

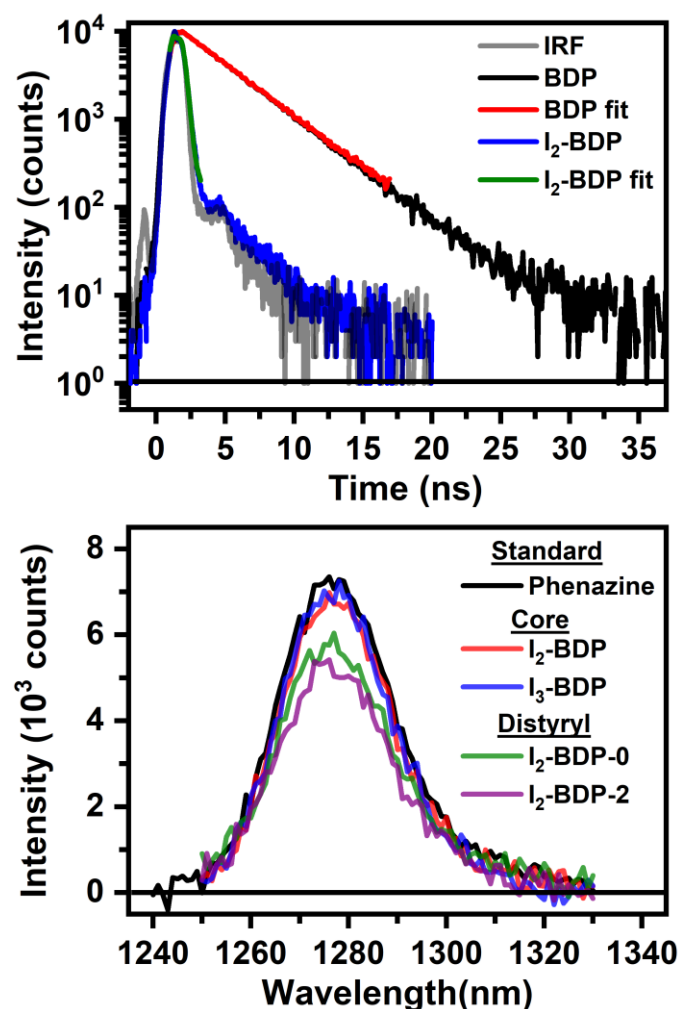


Figure 3. (Top) Fluorescence lifetime decays for **BDP** and **I₂-BDP** collected in aerated toluene. Representative fits are provided for each decay curve. (Bottom) Photosensitized singlet oxygen phosphorescence spectra collected from absorbance matched solutions of **I₂-BDP**, **I₃-BDP**, **I₂-**

BDP-0, and **I₂-BDP-2** in aerated toluene. The photosensitized singlet oxygen phosphorescence of the BDP derivatives is presented relative to a standard solution containing phenazine.

The four distyryl-BDP chromophores lacking iodine substitution in the 2- and 6- positions undergo no detectable intersystem crossing. The fluorescence quantum yields obtained for all of these distyryl-BDP derivatives (> 0.70) are greater than those obtained for the core BDPs (0.44 and 0.45) without iodine atoms in the 2- and 6- positions. The lifetime values obtained for the non-2,6-iodinated distyryl-BDPs agree within error (~ 5.50 ns) and are all appreciably longer than the lifetime values obtained for the non-2,6-iodinated core BDPs (3.20-3.80 ns). A rate constant analysis of these four, non-triplet forming distyryl-extended derivatives yields some interesting observations. The radiative decay rate constant for all of the derivatives is approximately $1.4 \times 10^8 \text{ s}^{-1}$. This value is nearly identical to the radiative decay rate constants obtained for the non-extended BDP chromophores. The non-radiative decay rate constants obtained for the non-triplet forming distyryl-extended BDP derivatives range from 2.8×10^7 to $5.0 \times 10^7 \text{ s}^{-1}$. These rates of non-radiative decay are at least a factor of two slower than those obtained for the non-extended BDP complexes; these smaller k_{nr} values result in the observed fluorescence quantum yield enhancement. The additional iodine atom in the *para-meso*-phenyl position results in a slight increase in the non-radiative decay rate constant and has no appreciable effect on the rate of intersystem crossing. This mirrors the effect of iodine substitution in the *para-meso*-phenyl position of the core BDP chromophores.

In contrast, both distyryl-BDP chromophores with iodine substitution in the 2- and 6- positions undergo appreciable intersystem crossing. **I₂-BDP-0** and **I₂-BDP-2** possess similar fluorescence quantum yields (~ 0.22), fluorescence lifetimes (1.70 ns), and high intersystem crossing quantum yields (~ 0.77). Radiative decay rate constants calculated for **I₂-BDP-0** and **I₂-BDP-2** are identical – $1.3 \times 10^8 \text{ s}^{-1}$. This k_r value is in agreement with the four core and four non-triplet forming distyryl-extended BDP derivatives. These derivatives appear to exhibit the lowest rates of k_{nr} in the series. However, the calculation of the exact non-radiative decay rate constants for **I₂-BDP-0** and **I₂-BDP-2** is complicated by the fact that radiative decay and intersystem crossing are efficient in these chromophores. No k_{nr} value is reported in **Table 2** for **I₂-BDP-0** as the sum of the fluorescence quantum yield and intersystem crossing quantum yield is 1. For **I₂-BDP-2**, the sum of the fluorescence quantum yield and intersystem crossing quantum yield is 0.99, resulting in a calculated value of k_{nr} of $5.9 \times 10^6 \text{ s}^{-1}$. The kinetic rates of intersystem crossing for **I₂-BDP-0** and **I₂-BDP-2** are also nearly identical with values of 4.5×10^8 and $4.6 \times 10^8 \text{ s}^{-1}$, respectively. These k_{ISC} values are notably an order of magnitude slower than in the triplet forming core BDPs, **I₂-BDP** and **I₃-BDP**. Intersystem crossing remains the dominant pathway due to the aforementioned diminished non-radiative decay in the distyryl-extended BDP derivatives. Nearly identical photophysical properties observed between **I₂-BDP-0** and **I₂-BDP-2** indicate iodination at the extended styryl-positions results in negligible effects upon the excited-state dynamics. This result is consistent with similar calculated rate constants for **BDP-0** and **I-BDP-0** when compared against **BDP-2** and **I-BDP-2**, respectively. The negligible effect of iodination at the *para*-styryl position of

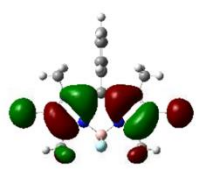
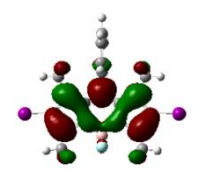
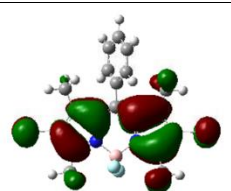
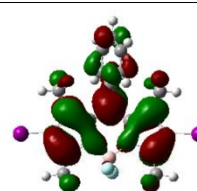
these extended BDP dyes suggests that orthogonal functionalization may be achieved without drastically changing the excited-state dynamics of the chromophore.

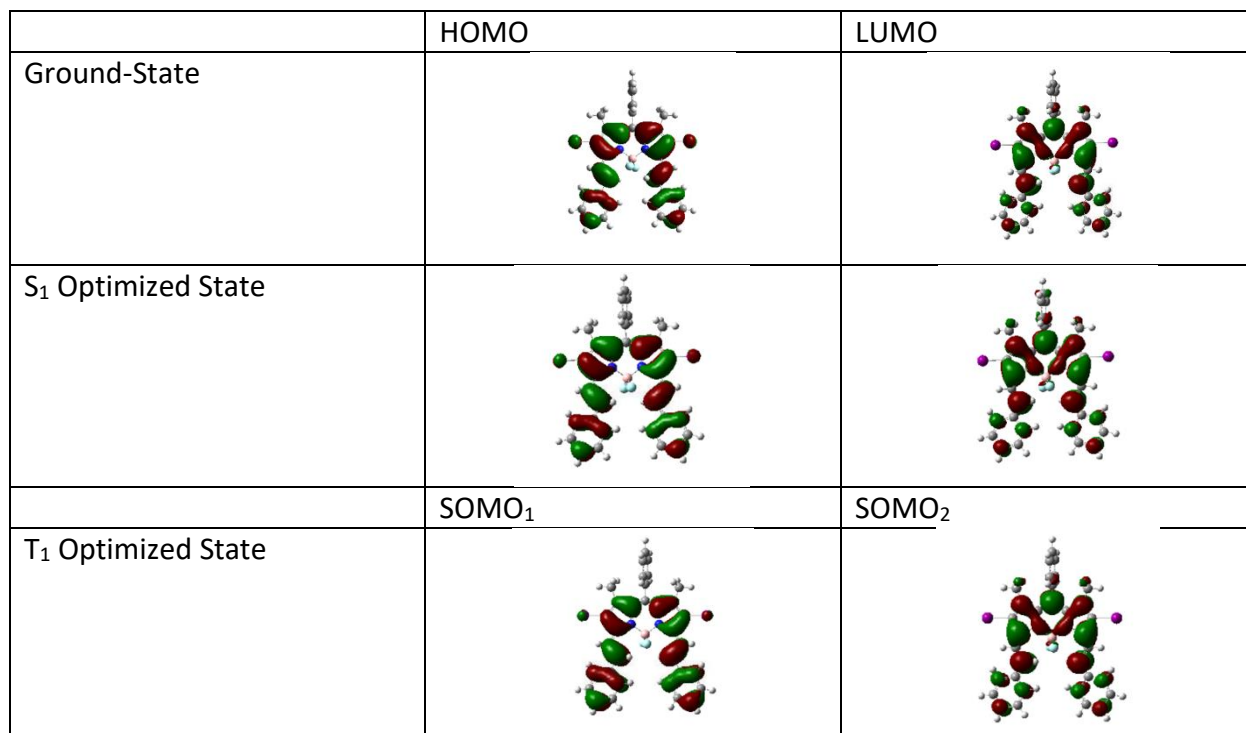
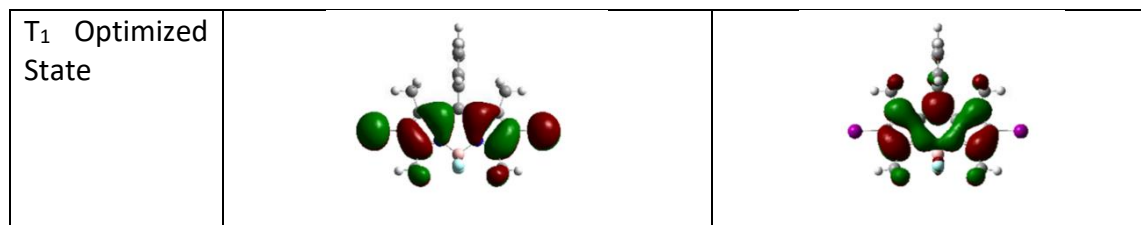
Electronic and Structural Factors Governing Intersystem Crossing and Vibrational Relaxation

DFT and TD-DFT calculations were performed on all ten derivatives in order to supplement our experimental data and to aid a discussion on the electronic and structural factors governing the rates of intersystem crossing in these chromophores. The calculated frontier molecular orbitals (HOMO, LUMO, SOMO₁, and SOMO₂) for **I₂-BDP** and **I₂-BDP-0** are shown in **Table 3**. Depictions of the frontier orbitals for the remaining derivatives are provided in **Tables S1-S10**. The calculated singlet-state energies, oscillator strengths, triplet-state energies, and singlet-triplet gaps are given in **Table S11**. The spin density plots for **I₂-BDP** and **I₂-BDP-0** are shown in **Table S12**. The calculated spin density residing on the individual iodine atoms in the triplet-state is tabulated in **Table S13**. Ground-state, singlet-state, and triplet-state geometry data are cataloged in **Tables S14-S15**.

The adiabatic energy difference (ΔE_{ST}) between the singlet excited-state (S_1) and the triplet excited-state (T_1) and spin density contributions from heavy atoms in the S_1 and T_1 excited-states can influence the rate of intersystem crossing (k_{ISC} in **Table 2**). Relative geometric distortions in the S_1 and T_1 excited-states can also play an important role in determining the rate of intersystem crossing (k_{ISC} in **Table 2**) as well as the rate of vibrational relaxation between the S_1 excited-state and the ground-state of the molecule (k_{nr} in **Table 2**).⁶²⁻⁶⁵ El-Sayed spin-orbit coupling (SOC) is not considered as a possible intersystem crossing pathway in these chromophores, as the S_1 and T_1 states in these molecules are both π - π^* in character. The π - π^* nature of these orbitals is supported by the presence of structured fluorescence and 77 K phosphorescence spectra (**Figure 2**) as well as DFT calculations.

Table 3. HOMO, LUMO, and SOMO molecular orbitals obtained from DFT calculations for (top) **I₂-BDP** and (bottom) **I₂-BDP-0**.

	HOMO	LUMO
Ground-State		
S_1 Optimized State		
	SOMO1	SOMO2



The magnitude of the adiabatic energy difference directly influences the rate of intersystem crossing with smaller values of ΔE_{ST} generally resulting in faster rates of intersystem crossing. The adiabatic energy difference between the S₁ and T₁ excited-states was obtained either spectroscopically or from DFT calculations. A comparison of the fluorescence and phosphorescence maxima of the four core BDP derivatives showed that the non-2,6-diiodo substituted derivatives, **BDP** and **I-BDP**, possess 0.18 eV larger singlet-triplet energy gaps than the 2,6-diiodo substituted derivatives, **I₂-BDP** and **I₃-BDP**. These experimental observations agree with the calculated singlet-triplet energy gaps of the four core BDP derivatives, which predict that the non-2,6-diiodo substituted derivatives possess 0.12 – 0.13 eV larger singlet-triplet energy gaps than the 2,6-diiodo substituted derivatives. Unfortunately, we were unable to obtain phosphorescence spectra for any of the distyryl-extended derivatives, prohibiting the spectroscopic determination of the T₁ energy. However, analysis of the calculated singlet-triplet

energy gaps of the distyryl-extended derivatives shows that the non-2,6-diiodo substituted derivatives, **BDP-0**, **I-BDP-0**, **BDP-2**, and **I-BDP-2**, possess nearly identical energy gaps, which are all at least 0.09 eV larger than the singlet-triplet energy gaps of the 2,6-diiodo substituted derivatives, **I₂-BDP-0** and **I₂-BDP-2**. The smaller adiabatic energy differences between the singlet and triplet excited-states of the 2,6-diiodo derivatives relative to the non-2,6-diiodo derivatives suggests that the rate of intersystem crossing will be faster in the 2,6-diiodo derivatives, in agreement with our experimental results.

The results of the DFT calculations also provide insight into the extent of heavy atom induced spin-orbit coupling in a particular BDP derivative through analysis of the relative amount of spin density located on the iodine atoms in the S_1 and T_1 states. A population analysis of the HOMO and LUMO of the ground and optimized S_1 states of all four 2,6-diiodo substituted derivatives, **I₂-BDP**, **I₃-BDP**, **I₂-BDP-0** and **I₂-BDP-2**, have < 5% electron density on the iodine atoms. The T_1 states of these molecules all have some calculated spin density on the iodine atoms in the 2- and 6-positions, while the magnitude of spin density on the iodine atom depends on the derivative. The relative amount of triplet spin density located on the iodine atoms is greater in the two core substituted derivatives, **I₂-BDP** and **I₃-BDP**, than in the distyryl-extended derivatives, **I₂-BDP-0** and **I₂-BDP-2**. This observation suggests that the magnitude of heavy atom induced spin-orbit coupling is greater in the core BDP derivatives than in the distyryl-extended BDP derivatives. These observations provide a second explanation for the higher rates of intersystem crossing in the core BDP derivatives compared to the distyryl-extended BDP derivatives. Furthermore, the presence of appreciable spin density on the iodine atoms in the core and distyryl-extended 2,6-diiodo derivatives provides an additional explanation for the observation of intersystem crossing in the 2,6-diiodo derivatives and not in the non-2,6-diiodo derivatives.

Excited-state geometry changes can lead to strong coupling of the singlet and triplet excited-state potential energy surfaces and enhance the rate of intersystem crossing. An analysis of the changes in planarity of BDP as well as changes in the dihedral angle between the plane of the styryl units and the plane of the BDP core (distyryl angle) and/or the dihedral angle between the plane of the *meso*-phenyl substituent and the plane of the BDP core (*meso*-phenyl angle) of **I₂-BDP**, **I₃-BDP**, **I₂-BDP-0** and **I₂-BDP-2** serves as a partial demonstration of the excited-state geometry changes in these chromophores (**Table S14**). There is significant puckering of the BDP backbone in the S_1 excited-states of **I₂-BDP** and **I₃-BDP**. The *meso*-carbon deflects 13.7° out of plane in **I₂-BDP** and 8.7° out of plane in **I₃-BDP** (**Table S15**). The geometry at the *meso*-carbon is drastically different in the S_1 excited-state than in the T_1 excited-state. In both **I₂-BDP** and **I₃-BDP**, the BDP core is planar in the T_1 excited-state (0° deflection, **Table S15**). The *meso*-phenyl angles in the geometry optimized singlet excited-states of **I₂-BDP** and **I₃-BDP** are 61.5° and 67.4°, respectively. In the geometry optimized triplet excited-states of the core BDP derivatives, the phenyl substituent is more rotated out of the plane of the BDP core, resulting in *meso*-phenyl angles of 79.8° in **I₂-BDP** and 90.0° in **I₃-BDP**. There is also puckering of the BDP backbone in the S_1 excited-states of **I₂-BDP-0** and **I₂-BDP-2**. The *meso*-carbon deflects 10.2° out of plane in **I₂-BDP-0** and 10.1° out of plane in **I₂-BDP-2** (**Table S15**). The geometry changes at the *meso*-carbon are

more subtle in the T_1 excited-states of the distyryl-extended derivatives with the *meso*-carbon deflected 8.5° and 8.8° out of plane in **I₂-BDP-0** and **I₂-BDP-2**, respectively. The *meso*-phenyl angle in the geometry optimized singlet excited-state of **I₂-BDP-0** is calculated to be 73.1° and that of **I₂-BDP-2** is calculated to be 74.1° . The phenyl substituent also rotates out of the plane of the BDP core in the geometry optimized triplet excited-states of the distyryl-extended BDPs. The calculated *meso*-phenyl angle in the triplet excited-state of **I₂-BDP-0** is 79.8° and 79.9° in **I₂-BDP-2**. A slight twist in the distyryl angle is expected when transitioning from the geometry optimized singlet excited-state to the geometry optimized triplet excited-state of the distyryl-extended BDP derivatives. The distyryl angle of **I₂-BDP-0** is calculated to be 10.8° in the geometry optimized singlet excited-state and 9.5° in the geometry optimized triplet excited-. The distyryl angle of **I₂-BDP-2** is calculated to be 11.2° in the geometry optimized singlet excited-state 9.7° in the geometry optimized triplet excited-state. This analysis demonstrates that the expected geometry changes between the S_1 and T_1 excited-states are attenuated in the distyryl-extended BDP derivatives relative to the core BDP derivatives. This diminished nuclear displacement suggests that the S_1 and T_1 potential energy surfaces are more nested in the distyryl-extended BDP derivatives than in the core BDP derivatives. In this regard, the distyryl-extended BDP derivatives tend towards the weak vibrational coupling limit, while the core BDP derivatives tend towards the strong vibrational coupling limit. These excited-state geometry changes provide a potential third reason for the enhanced rates of intersystem crossing in the core BDP derivatives compared to the distyryl-extended BDP derivatives.

Similarly, substantial twisting of the *meso*-phenyl group and dislocation of the BDP backbone in the singlet excited-state relative to the ground-state can also enhance the rate of vibrational relaxation (k_{nr} in **Table 2**) in these chromophores. It has recently been shown that the S_1 to ground-state vibrational relaxation mechanism proceeds through a distorted intermediate structure in which the core BDP plane and the *meso*-phenyl substituent are twisted.⁶⁴ This internal conversion pathway has been shown to be inhibited through rigidification of the BDP core via π -expansion in distyryl-extended derivatives.⁶⁵ These observations are consistent with our experimental results and are corroborated by the DFT calculations. The *meso*-phenyl angles in the geometry optimized singlet excited-states of **I₂-BDP** and **I₃-BDP** are 61.5° and 67.4° , respectively, which are substantially twisted versus the *meso*-phenyl angles in the ground-state at 81.1° and 87.0° , respectively (**Table S14**). The *meso*-carbon deflects 13.7° out of plane in **I₂-BDP** and 8.7° out of plane in **I₃-BDP** (**Table S15**), while becoming more planar in the ground-state with a *meso*-carbon angle of 1.6° in both **I₂-BDP** and in **I₃-BDP**. For the distyryl derivatives, the *meso*-phenyl angle in the geometry optimized singlet excited-state of **I₂-BDP-0** is 73.1° and that of **I₂-BDP-2** is 74.1° . The magnitude of the twist in the *meso*-phenyl angle is diminished in the distyryl-extended BDPs compared to the core BDPs with a *meso*-phenyl angle in the geometry optimized ground-state of 79.1° for **I₂-BDP-0** and 78.9° for **I₂-BDP-2** (**Table S14**). There is also less distortion at the *meso*-carbon between S_1 and ground-state of the distyryl-extended BDPs than in the core BDPs. The *meso*-carbon deflects 10.2° out of plane in **I₂-BDP-0** and 10.1° out of plane in **I₂-BDP-2**. The BDP core becomes more planar in the ground-state with a *meso*-carbon angle of

2.8° in both **I₂-BDP-0** and 6.9° in **I₂-BDP-2** (Table S15). Again, the expected geometry changes between the S_1 and ground-states are attenuated in the distyryl-extended BDP derivatives relative to the core BDP derivatives. The reduced nuclear displacement suggests that the S_1 and ground-state potential energy surfaces are also more nested in the distyryl-extended BDP derivatives than in the core BDP derivatives. This detailed discussion only focuses on a comparison of the 2,6-diiodo derivatives. The same trend of less nuclear displacement in the *meso*-phenyl angle and *meso*-carbon is also observed when comparing the geometry optimized S_1 excited-state and ground-state of **BDP-0**, **I-BDP-0**, **BDP-2**, and **I-BDP-2** with **BDP** and **I-BDP**. With all of the distyryl-extended BDP derivatives tending towards the weak vibrational coupling limit relative to the core BDP derivatives, slower rates of vibrational relaxation (k_{nr} in Table 2) from S_1 to the ground-state are expected for the distyryl-extended BDP derivatives.

Photostability

The photostability of **BDP**, **I₂-BDP**, **BDP-0**, and **I₂-BDP-0** was evaluated using mounted LEDs as described in the supporting information. Briefly, solutions of the BDP dyes were prepared in toluene with absorbance values of 0.5-0.6 at the LED output wavelength. The power output of each LED was adjusted in order to achieve an irradiance of 3.98 mW/cm². A picture of the photoirradiation set-up is provided in Figure S35. The absorption spectra of **BDP**, **I₂-BDP**, **BDP-0**, and **I₂-BDP-0** as a function of irradiation time are shown in Figure S36. The absorption spectra of the chromophores were unchanged over the course of a six hour photoirradiation. The data suggest that the chromophores do not possess a high quantum yield photodecomposition pathway and that the 2,6-iodinated chromophores, **I₂-BDP** and **I₂-BDP-0**, are stable in the presence of the singlet oxygen generated during the photoirradiation.

Conclusions

Among this series of four core and six distyryl-extended BODIPY dyes, iodine loading, substitution position, and π -extension were shown to exert significant influence on the photophysical properties of these molecules, teaching valuable lessons regarding future chromophore design. Varying the iodine content in these ten BDP derivatives modulated the non-radiative and intersystem crossing rate constants, while the radiative rate constant was not significantly influenced. Notably, only the BODIPY chromophores with iodine atoms in the 2- and 6- positions undergo appreciable intersystem crossing to form triplet excited-states. The rate of intersystem crossing is found to be approximately an order of magnitude faster in the 2,6-iodinated core BDPs than in the 2,6-iodinated distyryl-extended BDPs. DFT calculations and 77K phosphorescence experiments reveal smaller adiabatic energy differences between the S_1 and T_1 excited-states of the 2,6-diiodo substituted derivatives as well as significant spin density on the iodine atoms in the T_1 states of the 2,6-diiodo species. The amount of spin density on the 2,6-iodine atoms is appreciably lower in the distyryl-extended BDP derivatives than in the core BDP derivatives. DFT calculations also reveal more significant geometric distortion between the S_1 and T_1 states of the core BDP derivatives than the distyryl-extended BDP derivatives. This combination of electronic and structural factors explains the observation of intersystem crossing in the 2,6-diiodo

derivatives as well as the discrepancy in the rate of intersystem crossing between the 2,6-iodinated core BDPs and the 2,6-iodinated distyryl-extended BDPs. Further increasing iodine content beyond the 2,6-positions does not appreciably increase intersystem crossing quantum yields. Inclusion of iodine in the *para-meso*-phenyl position slightly increases the rate of non-radiative decay, while iodination at the *para*-styryl position generally has negligible effects on the observed rate constants. This observation indicates that functionalization in the *para*-styryl position (i.e. covalent polymer/substrate tethering) may be achievable without significantly impacting the excited-state dynamics for a given application (i.e. TTA and $^1\text{O}_2$ sensitization for PDT using triplet forming distyryl-BDPs). Additionally, distyryl extension at the 3,5-methylene positions not only induces significant bathochromic shifts in the lowest energy ground-state absorption maximum and the fluorescence maximum of the BDP chromophores but also drastically decreases non-radiative decay rates. DFT calculations reveal that distyryl extension decreases non-radiative decay rates through the rigidification of the BODIPY core structure. Ultimately, this work demonstrates that increasing iodine content within a particular chromophore does not necessarily enhance intersystem crossing efficiency and provides insight into the competitive rate constants that define the excited-state dynamics and guide future chromophore design.

Conflicts of Interest

The authors have no conflicts to disclose.

Acknowledgements

This research was performed while Kayla F. Presley held an NRC Research Associateship award at the Air Force Research Laboratory. This work was supported by Air Force Research Laboratory through contract #FA8650-15-D-5405 awarded to UES, Inc. and by Defense Advanced Research Projects Agency (DARPA) contract #140D6318C0019.

Electronic Supplementary Information

Materials and methods section including the experimental details of all photochemical measurements and DFT calculations. Full synthetic details and ^1H NMR and high resolution LDI-MS of all ten chromophores. ^{13}C NMR and the ATR-FTIR spectrum of the newly synthesized derivative, I-BDP-0, and the ATR-FTIR spectrum of the newly synthesized derivative, I₂-BDP-2. Examples of photochemical data including excitation spectra, fluorescence lifetime measurements with fits, fluorescence quantum yield data including integration ranges, photosensitized singlet oxygen quantum yield data collected relative to a phenazine standard, and 77 K phosphorescence spectra of the four core BDP derivatives. Examples of DFT data including frontier orbitals depictions, calculated singlet-state energies, oscillator strengths, triplet-state energies, singlet-triplet gaps, the spin density residing on the individual iodine atoms in the triplet-state SOMO orbitals, and ground-state, singlet-state, and triplet-state geometry data.

Corresponding Author

*E-mail: tod.grusenmeyer.1@us.af.mil

ORCID Numbers

J.T. Ly: 0000-0001-9164-508X

K.F. Presley: 0000-0001-9091-3214

T.M. Cooper: 0000-0002-4635-8281

L.A. Baldwin: 0000-0002-7787-238X

T.A. Grusenmeyer: 0000-0002-1842-056X

References

- 1 T. Yogo, Y. Urano, Y. Ishitsuka, F. Maniwa and T. Nagano, Highly Efficient and Photostable Photosensitizer Based on BODIPY Chromophore, *J. Am. Chem. Soc.*, 2005, **127**, 12162–12163.
- 2 A. Loudet and K. Burgess, BODIPY Dyes and Their Derivatives: Syntheses and Spectroscopic Properties, *Chem. Rev.*, 2007, **107**, 4891–4932.
- 3 B. Hinkeldey, A. Schmitt and G. Jung, Comparative Photostability Studies of BODIPY and Fluorescein Dyes by Using Fluorescence Correlation Spectroscopy, *ChemPhysChem*, 2008, **9**, 2019–2027.
- 4 C. S. Kue, S. Y. Ng, S. H. Voon, A. Kamkaew, L. Y. Chung, L. V. Kiew and H. B. Lee, Recent strategies to improve boron dipyrromethene (BODIPY) for photodynamic cancer therapy: an updated review, *Photochem. Photobiol. Sci.*, 2018, **17**, 1691–1708.
- 5 W. Sun, X. Zhao, J. Fan, J. Du and X. Peng, Boron Dipyrromethene Nano-Photosensitizers for Anticancer Phototherapies, *Small*, 2019, **15**, 1804927.
- 6 T. Zhang, C. Ma, T. Sun and Z. Xie, Unadulterated BODIPY nanoparticles for biomedical applications, *Coord. Chem. Rev.*, 2019, **390**, 76–85.
- 7 J. Wang, Q. Gong, L. Wang, E. Hao and L. Jiao, The main strategies for tuning BODIPY fluorophores into photosensitizers, *J. Porphy. Phthalocyanines*, 2019, **24**, 603–635.
- 8 M. A. Filatov, S. Karuthedath, P. M. Polestshuk, H. Savoie, K. J. Flanagan, C. Sy, E. Sitte, M. Telitchko, F. Laquai, R. W. Boyle and M. O. Senge, Generation of Triplet Excited States via Photoinduced Electron Transfer in meso-anthra-BODIPY: Fluorogenic Response toward Singlet Oxygen in Solution and in Vitro, *J. Am. Chem. Soc.*, 2017, **139**, 6282–6285.
- 9 M. A. Filatov, Heavy-atom-free BODIPY photosensitizers with intersystem crossing

- mediated by intramolecular photoinduced electron transfer, *Org. Biomol. Chem.*, 2020, **18**, 10–27.
- 10 S. G. Awuah and Y. You, Boron dipyrromethene (BODIPY)-based photosensitizers for photodynamic therapy, *RSC Adv.*, 2012, **2**, 11169–11183.
 - 11 A. Kamkaew, S. H. Lim, H. B. Lee, L. V. Kiew, L. Y. Chung and K. Burgess, BODIPY dyes in photodynamic therapy, *Chem. Soc. Rev.*, 2013, **42**, 77–88.
 - 12 J. Zhao, K. Xu, W. Yang, Z. Wang and F. Zhong, The triplet excited state of Bodipy: formation, modulation and application, *Chem. Soc. Rev.*, 2015, **44**, 8904–8939.
 - 13 J. Zhao, K. Chen, Y. Hou, Y. Che, L. Liu and D. Jia, Recent progress in heavy atom-free organic compounds showing unexpected intersystem crossing (ISC) ability, *Org. Biomol. Chem.*, 2018, **16**, 3692–3701.
 - 14 X. Cui, J. Zhao, Z. Mohmood and C. Zhang, Accessing the Long-Lived Triplet Excited States in Transition-Metal Complexes: Molecular Design Rationales and Applications, *Chem. Rec.*, 2016, **16**, 173–188.
 - 15 B. Bertrand, K. Passador, C. Goze, F. Denat, E. Bodio and M. Salmain, Metal-based BODIPY derivatives as multimodal tools for life sciences, *Coord. Chem. Rev.*, 2018, **358**, 108–124.
 - 16 A. M. Durantini, D. A. Heredia, J. E. Durantini and E. N. Durantini, BODIPYs to the rescue: Potential applications in photodynamic inactivation, *Eur. J. Med. Chem.*, 2018, **144**, 651–661.
 - 17 A. Turksoy, D. Yildiz and E. U. Akkaya, Photosensitization and controlled photosensitization with BODIPY dyes, *Coord. Chem. Rev.*, 2019, **379**, 47–64.
 - 18 W. Wu, X. Cui and J. Zhao, Hetero Bodipy-dimers as heavy atom-free triplet photosensitizers showing a long-lived triplet excited state for triplet–triplet annihilation upconversion, *Chem. Commun.*, 2013, **49**, 9009–9011.
 - 19 W. Wu, J. Zhao, H. Guo, J. Sun, S. Ji and Z. Wang, Long-Lived Room-Temperature Near-IR Phosphorescence of BODIPY in a Visible-Light-Harvesting N^CN PtII–Acetylide Complex with a Directly Metalated BODIPY Chromophore, *Chem. – A Eur. J.*, 2012, **18**, 1961–1968.
 - 20 X. Yi, J. Zhao, J. Sun, S. Guo and H. Zhang, Visible light-absorbing rhenium(i) tricarbonyl complexes as triplet photosensitizers in photooxidation and triplet–triplet annihilation upconversion, *Dalt. Trans.*, 2013, **42**, 2062–2074.
 - 21 W. Wu, J. Zhao, J. Sun, L. Huang and X. Yi, Red-light excitable fluorescent platinum(ii) bis(aryleneethynylene) bis(trialkylphosphine) complexes showing long-lived triplet excited states as triplet photosensitizers for triplet–triplet annihilation upconversion, *J. Mater. Chem. C*, 2013, **1**, 705–716.
 - 22 H. Jia, B. Küçüköz, Y. Xing, P. Majumdar, C. Zhang, A. Karatay, G. Yaglioglu, A. Elmali, J. Zhao and M. Hayvali, trans-Bis(alkylphosphine) platinum(ii)-alkynyl complexes showing

- broadband visible light absorption and long-lived triplet excited states, *J. Mater. Chem. C*, 2014, **2**, 9720–9736.
- 23 K. T. Chan, G. S. M. Tong, W. P. To, C. Yang, L. Du, D. L. Phillips and C. M. Che, The interplay between fluorescence and phosphorescence with luminescent gold(i) and gold(iii) complexes bearing heterocyclic arylacetylide ligands, *Chem. Sci.*, 2017, **8**, 2352–2364.
- 24 L. Huang, J. Zhao, S. Guo, C. Zhang and J. Ma, Bodipy Derivatives as Organic Triplet Photosensitizers for Aerobic Photoorganocatalytic Oxidative Coupling of Amines and Photooxidation of Dihydroxynaphthalenes, *J. Org. Chem.*, 2013, **78**, 5627–5637.
- 25 P. Irmeler and R. F. Winter, Complexes trans-Pt(BODIPY)X(PEt₃)₂: excitation energy-dependent fluorescence and phosphorescence emissions, oxygen sensing and photocatalysis, *Dalt. Trans.*, 2016, **45**, 10420–10434.
- 26 W. Li, L. Li, H. Xiao, R. Qi, Y. Huang, Z. Xie, X. Jing and H. Zhang, Iodo-BODIPY: a visible-light-driven, highly efficient and photostable metal-free organic photocatalyst, *RSC Adv.*, 2013, **3**, 13417–13421.
- 27 J. Zou, Z. Yin, K. Ding, Q. Tang, J. Li, W. Si, J. Shao, Q. Zhang, W. Huang and X. Dong, BODIPY Derivatives for Photodynamic Therapy: Influence of Configuration versus Heavy Atom Effect, *ACS Appl. Mater. Interfaces*, 2017, **9**, 32475–32481.
- 28 M. J. Ortiz, A. R. Agarrabeitia, G. Duran-Sampedro, J. Bañuelos Prieto, T. A. Lopez, W. A. Massad, H. A. Montejano, N. A. García and I. Lopez Arbeloa, Synthesis and functionalization of new polyhalogenated BODIPY dyes. Study of their photophysical properties and singlet oxygen generation, *Tetrahedron*, 2012, **68**, 1153–1162.
- 29 N. Adarsh, M. Shanmugasundaram, R. R. Avirah and D. Ramaiah, Aza-BODIPY Derivatives: Enhanced Quantum Yields of Triplet Excited States and the Generation of Singlet Oxygen and their Role as Facile Sustainable Photooxygenation Catalysts, *Chem. – A Eur. J.*, 2012, **18**, 12655–12662.
- 30 Y. Cakmak, S. Kolemen, S. Duman, Y. Dede, Y. Dolen, B. Kilic, Z. Kostereli, L. T. Yildirim, A. L. Dogan, D. Guc and E. U. Akkaya, Designing Excited States: Theory-Guided Access to Efficient Photosensitizers for Photodynamic Action, *Angew. Chemie Int. Ed.*, 2011, **50**, 11937–11941.
- 31 S. Duman, Y. Cakmak, S. Kolemen, E. U. Akkaya and Y. Dede, Heavy Atom Free Singlet Oxygen Generation: Doubly Substituted Configurations Dominate S₁ States of Bis-BODIPYs, *J. Org. Chem.*, 2012, **77**, 4516–4527.
- 32 W. Pang, X.-F. Zhang, J. Zhou, C. Yu, E. Hao and L. Jiao, Modulating the singlet oxygen generation property of meso-β directly linked BODIPY dimers, *Chem. Commun.*, 2012, **48**, 5437–5439.
- 33 A. N. Amin, M. E. El-Khouly, N. K. Subbaiyan, M. E. Zandler, S. Fukuzumi and F. D'Souza, A novel BF₂-chelated azadipyromethene–fullerene dyad: synthesis, electrochemistry and

- photodynamics, *Chem. Commun.*, 2012, **48**, 206–208.
- 34 L. Huang, X. Yu, W. Wu and J. Zhao, Styryl Bodipy-C60 Dyads as Efficient Heavy-Atom-Free Organic Triplet Photosensitizers, *Org. Lett.*, 2012, **14**, 2594–2597.
- 35 P. Yang, W. Wu, J. Zhao, D. Huang and X. Yi, Using C60-bodipy dyads that show strong absorption of visible light and long-lived triplet excited states as organic triplet photosensitizers for triplet–triplet annihilation upconversion, *J. Mater. Chem.*, 2012, **22**, 20273–20283.
- 36 W. Wu, J. Zhao, J. Sun and S. Guo, Light-Harvesting Fullerene Dyads as Organic Triplet Photosensitizers for Triplet–Triplet Annihilation Upconversions, *J. Org. Chem.*, 2012, **77**, 5305–5312.
- 37 L. Huang, X. Cui, B. Therrien and J. Zhao, Energy-Funneling-Based Broadband Visible-Light-Absorbing Bodipy–C60 Triads and Tetrads as Dual Functional Heavy-Atom-Free Organic Triplet Photosensitizers for Photocatalytic Organic Reactions, *Chem. – A Eur. J.*, 2013, **19**, 17472–17482.
- 38 A. A. Rachford, R. Ziessel, T. Bura, P. Retailleau and F. N. Castellano, Boron Dipyrromethene (Bodipy) Phosphorescence Revealed in $[\text{Ir}(\text{ppy})_2(\text{bpy}-\text{C}\equiv\text{C}-\text{Bodipy})]^+$, *Inorg. Chem.*, 2010, **49**, 3730–3736.
- 39 W. Wu, J. Sun, X. Cui and J. Zhao, Observation of the room temperature phosphorescence of Bodipy in visible light-harvesting Ru(ii) polyimine complexes and application as triplet photosensitizers for triplet–triplet-annihilation upconversion and photocatalytic oxidation, *J. Mater. Chem. C*, 2013, **1**, 4577–4589.
- 40 J. Wang, Y. Lu, N. McGoldrick, C. Zhang, W. Yang, J. Zhao and S. M. Draper, Dual phosphorescent dinuclear transition metal complexes, and their application as triplet photosensitizers for TTA upconversion and photodynamic therapy, *J. Mater. Chem. C*, 2016, **4**, 6131–6139.
- 41 J. Sun, F. Zhong, X. Yi and J. Zhao, Efficient Enhancement of the Visible-Light Absorption of Cyclometalated Ir(III) Complexes Triplet Photosensitizers with Bodipy and Applications in Photooxidation and Triplet–Triplet Annihilation Upconversion, *Inorg. Chem.*, 2013, **52**, 6299–6310.
- 42 P. Majumdar, X. Yuan, S. Li, B. Le Guennic, J. Ma, C. Zhang, D. Jacquemin and J. Zhao, Cyclometalated Ir(iii) complexes with styryl-BODIPY ligands showing near IR absorption/emission: preparation, study of photophysical properties and application as photodynamic/luminescence imaging materials, *J. Mater. Chem. B*, 2014, **2**, 2838–2854.
- 43 E. Palao, R. Sola-Llano, A. Tabero, H. Manzano, A. R. Agarrabeitia, A. Villanueva, I. López-Arbeloa, V. Martínez-Martínez and M. J. Ortiz, AcetylacetonateBODIPY-Biscyclometalated Iridium(III) Complexes: Effective Strategy towards Smarter Fluorescent Photosensitizer Agents, *Chem. – A Eur. J.*, 2017, **23**, 10139–10147.
- 44 L. Tabrizi and H. Chiniforoshan, New cyclometalated Ir(iii) complexes with NCN pincer

- and meso-phenylcyanamide BODIPY ligands as efficient photodynamic therapy agents, *RSC Adv.*, 2017, **7**, 34160–34169.
- 45 K. S. Choung, K. Marroquin and T. S. Teets, Cyclometalated iridium–BODIPY ratiometric O₂ sensors, *Chem. Sci.*, 2019, **10**, 5124–5132.
- 46 F. Geist, A. Jackel and R. F. Winter, Ligand Based Dual Fluorescence and Phosphorescence Emission from BODIPY Platinum Complexes and Its Application to Ratiometric Singlet Oxygen Detection, *Inorg. Chem.*, 2015, **54**, 10946–10957.
- 47 W. Yang, A. Karatay, J. Zhao, J. Song, L. Zhao, Y. Xing, C. Zhang, C. He, H. G. Yaglioglu, M. Hayvali, A. Elmali and B. Küçüköz, Near-IR Broadband-Absorbing trans-Bisphosphine Pt(II) Bisacetylide Complexes: Preparation and Study of the Photophysics, *Inorg. Chem.*, 2015, **54**, 7492–7505.
- 48 V. Ramu, S. Gautam, A. Garai, P. Kondaiah and A. R. Chakravarty, Glucose-Appended Platinum(II)-BODIPY Conjugates for Targeted Photodynamic Therapy in Red Light, *Inorg. Chem.*, 2018, **57**, 1717–1726.
- 49 M. Üçüncü, E. Karakuş, E. Kurulgan Demirci, M. Sayar, S. Dartar and M. Emrullahoğlu, BODIPY–Au(I): A Photosensitizer for Singlet Oxygen Generation and Photodynamic Therapy, *Org. Lett.*, 2017, **19**, 2522–2525.
- 50 A. Maity, A. Sarkar, A. Sil, S. B. B. N. and S. K. Patra, Synthesis, photophysical and concentration-dependent tunable lasing behavior of 2,6-diacetylenyl-functionalized BODIPY dyes, *New J. Chem.*, 2017, **41**, 2296–2308.
- 51 H. L. Kee, C. Kirmaier, L. Yu, P. Thamyongkit, W. J. Youngblood, M. E. Calder, L. Ramos, B. C. Noll, D. F. Bocian, W. R. Scheidt, R. R. Birge, J. S. Lindsey and D. Holten, Structural Control of the Photodynamics of Boron–Dipyrin Complexes, *J. Phys. Chem. B*, 2005, **109**, 20433–20443.
- 52 X. Yin, Y. Li, Y. Li, Y. Zhu, X. Tang, H. Zheng and D. Zhu, Electrochromism based on the charge transfer process in a ferrocene–BODIPY molecule, *Tetrahedron*, 2009, **65**, 8373–8377.
- 53 S. H. Lim, C. Thivierge, P. Nowak-Sliwinska, J. Han, H. van den Bergh, G. Wagnières, K. Burgess and H. B. Lee, In Vitro and In Vivo Photocytotoxicity of Boron Dipyrromethene Derivatives for Photodynamic Therapy, *J. Med. Chem.*, 2010, **53**, 2865–2874.
- 54 Y. Yan, F. Wu, J. Qin, H. Xu, M. Shi, J. Zhou, J. Mack, G. Fomo, T. Nyokong and Z. Shen, Efficient energy transfer in ethynyl bridged corrole–BODIPY dyads, *RSC Adv.*, 2016, **6**, 72852–72858.
- 55 R. Ziessel, T. Bura and J.-H. Olivier, Elaborating Boron Dipyrromethene Dyes with Conjugated Polyaromatic Frameworks, *Synlett*, 2010, **2010**, 2304–2310.
- 56 N. J. Turro, *Modern Molecular Photochemistry*, University Science Books, 1991.
- 57 Q. Zeng, F. Li, Z. Chen, K. Yang, Y. Liu, T. Guo, G.-G. Shan and Z.-M. Su, Rational Design of

- Efficient Organometallic Ir(III) Complexes for High-Performance Flexible Monochromatic and White Light-Emitting Electrochemical Cells, *ACS Appl. Mater. Interfaces*, 2020, **12**, 4649–4658.
- 58 C. Tahtaoui, C. Thomas, F. Rohmer, P. Klotz, G. Duportail, Y. Mély, D. Bonnet and M. Hibert, Convenient Method To Access New 4,4-Dialkoxy- and 4,4-Diaryloxy-diaza-s-indacene Dyes: Synthesis and Spectroscopic Evaluation, *J. Org. Chem.*, 2007, **72**, 269–272.
- 59 S. P. McGlynn, T. Azumi and M. Kinoshita, *Molecular Spectroscopy of the Triplet State*, Prentice-Hall, Inc., Englewood Cliffs, 1969.
- 60 S. P. McGlynn, J. Daigre and F. J. Smith, External Heavy-Atom Spin—Orbital Coupling Effect. IV. Intersystem Crossing, *J. Chem. Phys.*, 1963, **39**, 675–679.
- 61 H. Wang, M. G. H. Vicente, F. R. Fronczek and K. M. Smith, Synthesis and Transformations of 5-Chloro-2,2'-Dipyrrins and Their Boron Complexes, 8-Chloro-BODIPYs, *Chem. – A Eur. J.*, 2014, **20**, 5064–5074.
- 62 C. M. Marian, Spin–orbit coupling and intersystem crossing in molecules, *WIREs Comput. Mol. Sci.*, 2012, **2**, 187–203.
- 63 T. J. Penfold, E. Gindensperger, C. Daniel and C. M. Marian, Spin-Vibronic Mechanism for Intersystem Crossing, *Chem. Rev.*, 2018, **118**, 6975–7025.
- 64 Z. Lin, A. W. Kohn and T. Van Voorhis, Toward Prediction of Nonradiative Decay Pathways in Organic Compounds II: Two Internal Conversion Channels in BODIPYs, *J. Phys. Chem. C*, 2020, **124**, 3925–3938.
- 65 L. Gai, J. Mack, H. Lu, H. Yamada, D. Kuzuhara, G. Lai, Z. Li and Z. Shen, New 2,6-Distyryl-Substituted BODIPY Isomers: Synthesis, Photophysical Properties, and Theoretical Calculations, *Chem. – A Eur. J.*, 2014, **20**, 1091–1102.